Supplementary Information (SI) for Journal of Materials Chemistry C.

Supplementary Materials

Selector-only memory in Si-doped GeSeTe chalcogenide with superior endurance and memory window

Na Eun Kim [a], Min Kyu Yang [b, *], and Gun Hwan Kim [a,c, *]

a Department of System Semiconductor Engineering, Yonsei University, Seoul 03722, Republic of Korea

b Department of Artificial Intelligence Semiconductor Engineering, Sahmyook University, Seoul 01795, Republic of Korea

c Department of Materials Science and Engineering, Yonsei University, Seoul 03722, Republic of Korea

[*] Corresponding authors: dbrophd@syu.ac.kr (M. K. Yang), kgh@yonsei.ac.kr (G.H. Kim)

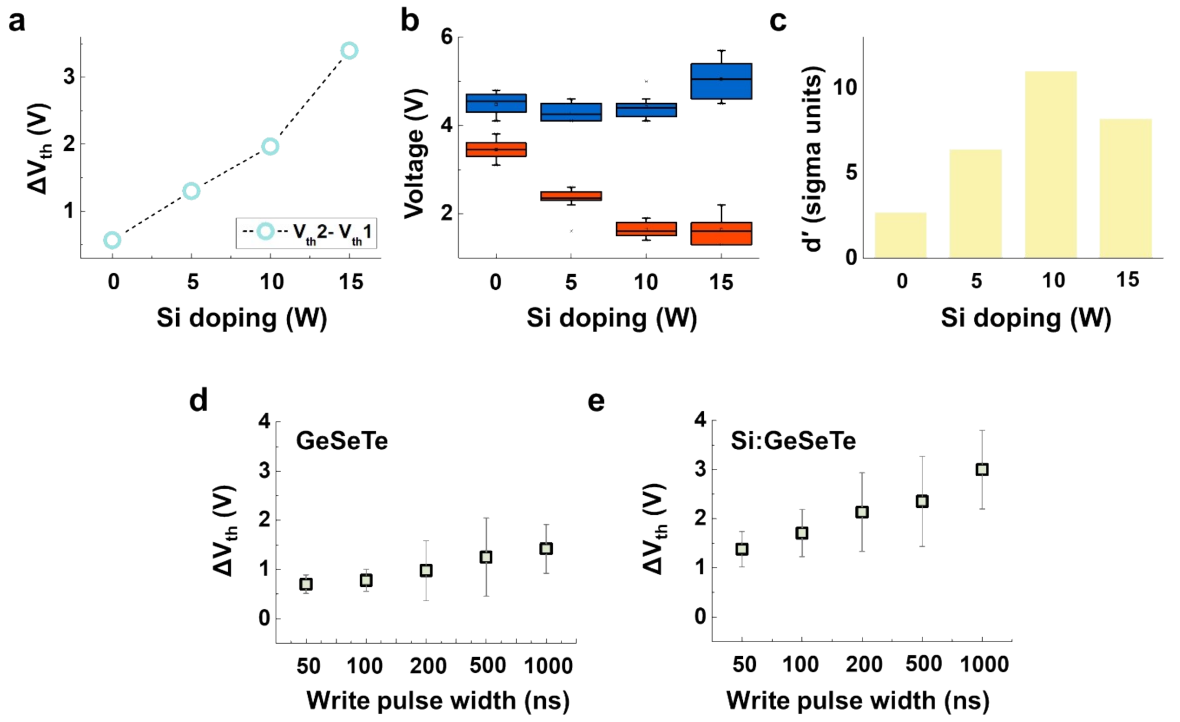

Fig. S1. (a–c) Optimization of Si doping power in GeSeTe films for selector-only memory devices. (a) Variation of threshold-voltage margin ($\Delta V_{th} = V_{th}2 - V_{th}1$) as a function of Si sputtering power. (b) Extracted V_{th1} and V_{th2} values for devices with different Si doping powers. (c) Evaluation of threshold overlap ($V_{th}1$–$V_{th}2$ intersection) showing that 10 W Si doping yields the optimal margin with minimal overlap. (d,e) Dependence of threshold voltages on write-pulse width for (d) GeSeTe and (e) Si:GeSeTe devices. A programming pulse width of 1000 ns was used for endurance and ΔV_{th} extraction in the main text.

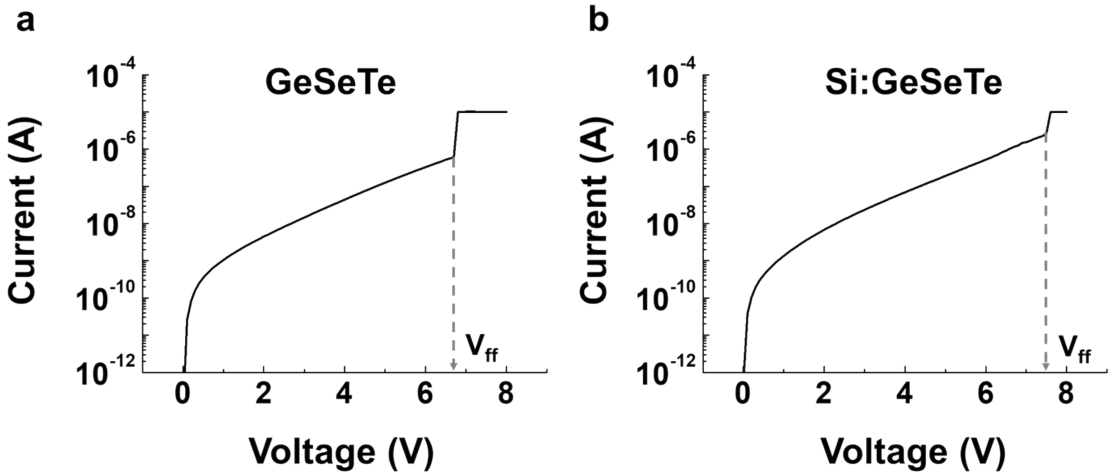

Fig. S2. Representative first-fire (FF) *I–V* curves of pristine (a) GeSeTe and (b) Si:GeSeTe SOM devices. FF measurements were carried out using a DC voltage sweep from 0 to 8 V with a step of 0.1 V under a compliance current of 10 μA. The first-fire voltage (V_{ff}) is indicated by the dashed arrows and was defined as the voltage at which the first abrupt current increase occurred during the initial activation of the pristine device.

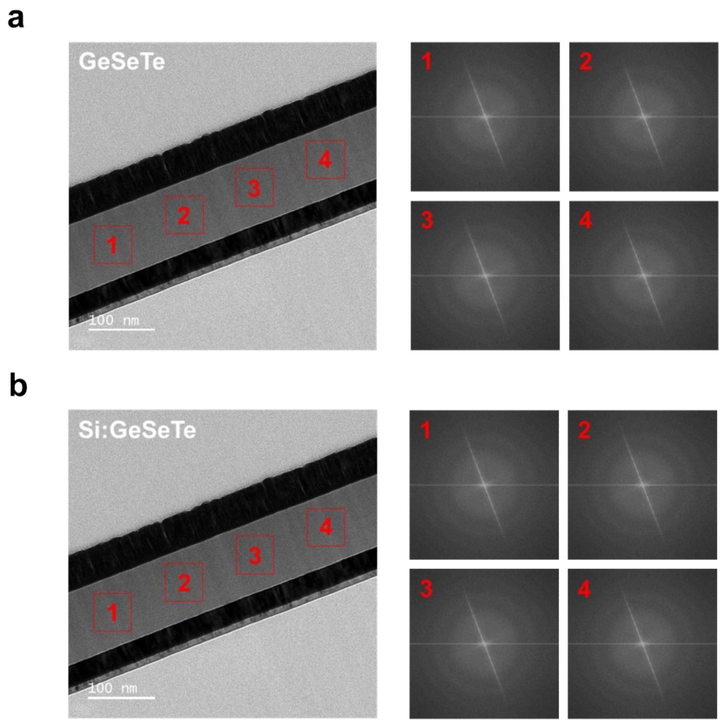

Fig. S3. Cross-sectional TEM images and local FFT analyses from multiple representative regions of the active layers in (a) GeSeTe and (b) Si:GeSeTe SOM devices. The numbered red boxes indicate the locations selected for local FFT analysis. All selected regions exhibit diffuse halo patterns without discrete diffraction spots, confirming the absence of local crystallization or phase separation and indicating that the amorphous structure is uniformly preserved in both active layers.

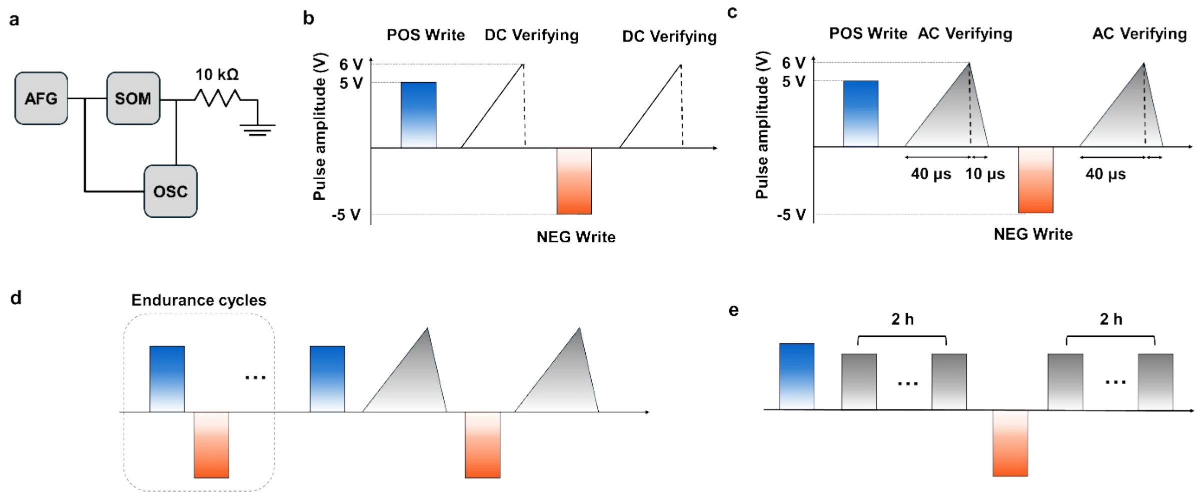

Fig. S4. Schematic diagrams of the electrical measurement setup and pulse sequences used for SOM characterization. (a) Electrical measurement setup for SOM devices. (b) DC read scheme for acquiring steady-state *I*–*V* curves. (c) Pulse read scheme for measuring transient switching behavior. (d) Endurance test scheme applying alternating positive and negative pulses to monitor V_{th} variation with cycle number. (e) Retention test scheme in which the device response is periodically monitored after a single programming pulse.

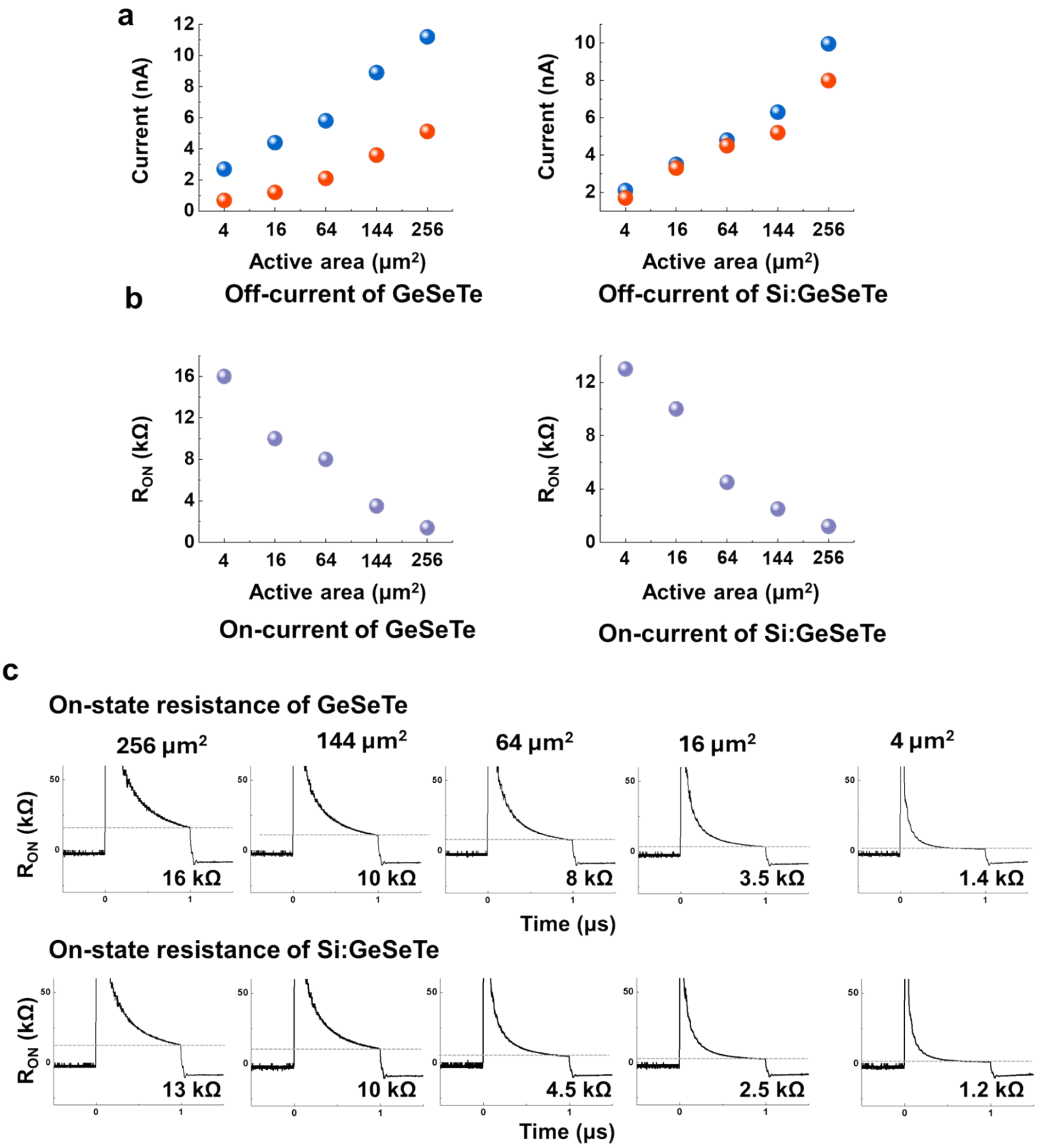

Fig. S5. (a) Off-state current (I_{off}) of the GeSeTe- and Si:GeSeTe-based SOM devices as a function of active area. Here, the off-current refers to the post-firing off-state current measured after the firing process. (b) On-state resistance (RON) of the GeSeTe- and Si:GeSeTe-based SOM devices as a function of active area. (c) Measured R_{ON} values of individual devices according to active area. The off-state current increases with active area, whereas the on-state resistance decreases as the active area increases. These area-dependent electrical characteristics are not consistent with a strictly localized single-filament conduction path under the present measurement conditions.

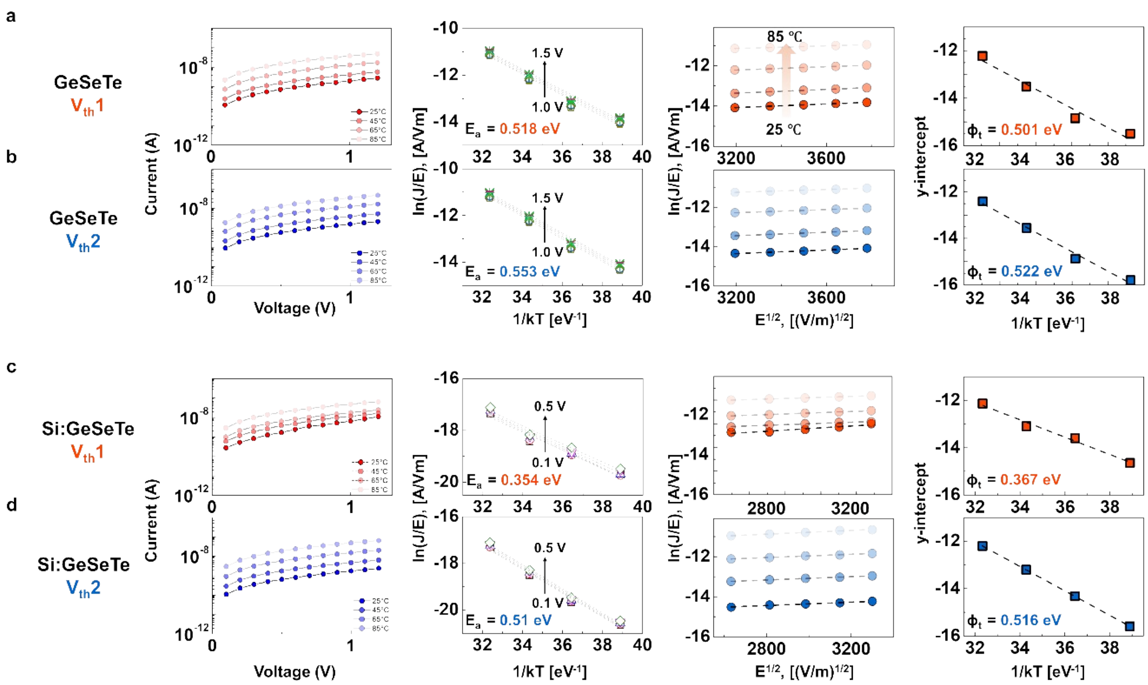

Fig. S6. Temperature-dependent conduction analysis of the GeSeTe- and Si:GeSeTe-based SOM devices in the two programmed states. The first and second rows correspond to the GeSeTe device in the $V_{th}1$ and $V_{th}2$ states, respectively, and the third and fourth rows correspond to the Si:GeSeTe device in the $V_{th}1$ and $V_{th}2$ states, respectively. From left to right, the panels show the temperature-dependent *I–V* characteristics, Arrhenius plots used to extract the activation energy (E_a), Poole–Frenkel plots of ln*(J/E)* versus $E^{1/2}$, and the corresponding y-intercept versus 1/kT plots used to extract the trap depth (Φ_t). The extracted E_a and Φ_t values are directly indicated in each fitting plot for clarity.

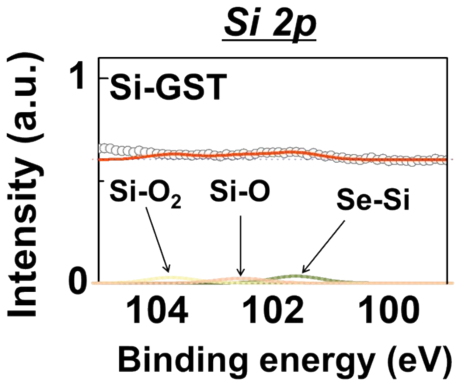

Fig. S7. XPS spectrum of the Si 2*p* region for Si:GeSeTe thin films. The fitted Si 2*p* peak corresponds mainly to Si–Se bonding, confirming successful Si incorporation into the amorphous GeSeTe matrix.